Reply to "Comment on the paper by Buono et al. "Dynamics of degassing in evolved alkaline magmas: Petrological, experimental and theoretical insights" (Earth Science Reviews, 211 (2020), 103402)"

Gianmarco Buono [a,b,*], Sara Fanara [c], Giovanni Macedonio [a], Danilo M. Palladino [d], Paola Petrosino [b], Gianluca Sottili [d], Lucia Pappalardo [a]

a - Istituto Nazionale di Geofisica e Vulcanologia, Sezione di Napoli - Osservatorio Vesuviano, Naples, Italy

b - University of Naples Federico II, Department of Earth, Environmental and Resources Science, Naples, Italy

c - Georg-August University of Göttingen, Department of Experimental and Applied Mineralogy, Göttingen, Germany

d – Sapienza-University of Rome, Department of Earth Sciences, Rome, Italy

* corresponding author e-mail address: gianmarco.buono@unina.it

Abstract

In our original paper (Buono et al., 2020), we investigated the dynamics of degassing (e.g., bubble nucleation and growth, degassing styles and regimes) of H_2O-, CO_2- and H_2O-CO_2-rich evolved alkaline melts over a wide range of variables (final pressures, decompression rates, volatile compositions and contents, temperatures) through a comprehensive review of previous and new HP (high pressure)-HT (high temperature) decompression experiments. The criticism of Allabar and Nowak regards a restricted part of our results, i.e., those concerning homogeneous bubble nucleation from our new experiments on H_2O-rich melts. Their aim is refusing the classical nucleation theory (CNT), widely accepted in literature to explain homogeneous bubble nucleation in magmas, for evolved alkaline melts in favour of the spinodal decomposition.

We found that the Authors of the Comment do not provide any new evidence in support of their thesis, but they keep only arbitrary and erroneous conjectures of our new experimental data. As we stated in our original paper, the evaluation of the specific bubble nucleation mechanism (CNT *vs.* spinodal decomposition) is beyond the scope of our research, as appropriate studies on both experimental and natural products would be necessary to shed light on this complex issue.

Keywords: alkaline melts; magma degassing; magma ascent

1. Introduction

In our paper (Buono et al., 2020) we investigated the dynamics of degassing in evolved alkaline magmas through a critical review of the available experimental works, and new HP (high pressure)-HT (high temperature) decompression experiments performed on purpose to fill the gap in the existing heterogeneous dataset. We explored systematically a wide range of final pressures (P_f from 200 to 10 MPa), decompression rates (dP/dt from 10^{-3} to 10 MPa s^{-1}), volatile compositions and contents (H_2O and CO_2), and temperatures (T from 800 to 1200 °C). Our results allowed, for the first time, to fully constrain the degassing behaviour (e.g., bubble nucleation and growth, degassing styles and regimes) of H_2O-, CO_2- and H_2O-CO_2-rich evolved alkaline melts.

Allabar and Nowak (this issue) raise criticism on part of our new experimental results, i.e., those related to homogeneous bubble nucleation of H_2O-rich melts, principally with the aim to contest the application of the classical nucleation theory (CNT) to alkaline melts. Actually, the CNT is widely accepted in literature to explain the homogeneous bubble nucleation in magmas (e.g., Sparks, 1978; 2003; Toramaru, 1995; Navon and Lyakhovsky, 1998; Gonnermann and Manga, 2007; 2012; for experimental evidence in evolved alkaline melts, see e.g., Iacono-Marziano et al., 2007; Gardner, 2012; Gardner et al., 2013). However, the Authors of the Comment proposed in previous papers (Allabar and Nowak, 2018; Allabar et al., 2020a) the spinodal decomposition as an alternative mechanism to CNT, to justify some of their decompression experimental results on bubble nucleation in phonolitic melts. In particular, they observed an independence of the bubble number density (*BND*) from the decompression rate (*dP/dt*) in some experimental samples, in contrast with the positive *BND vs. dP/dt* correlation predicted by the decompression rate meter of Toramaru (2006) based on the CNT.

In this regard, in our paper, we proposed an alternative explanation for the inconsistency of the Toramaru model in the case of some alkaline experimental samples. Specifically, we showed that the Toramaru model combines CNT with a specific diffusive bubble growth model, calibrated for rhyolitic melts only, whose approximations may not be suitable to reproduce the non-linear *BND vs. dP/dt* trends observed in some alkaline melts (due to their different diffusivity, viscosity, surface tension, etc.). However, we also point out that the evaluation of the specific bubble nucleation mechanism (CNT *vs.* spinodal decomposition) was beyond the focus of our paper and thus was only briefly considered in the Discussion (section 3.1.1.3).

We firmly think, as already stressed in our paper (last paragraph of section 3.1.1.3), that only new experimental studies, appropriately designed to address this complex issue, as well as new evidence from eruptive products, could clarify the conditions that may lead to different mechanisms of bubble nucleation in magmas. After all, the Authors of the Comment seem to agree with our view, as their Introduction and Conclusions actually report: "*The question, whether spinodal decomposition occurs in phonolitic (or in general in evolved alkaline melts) remains open*", thus making the purpose of their Comment unclear. In fact, they do not provide any kind of new evidence in support of their hypothesis, yet they keep only arbitrary and erroneous conjectures on part of our experimental procedures and results. In this Reply, we address in detail the points raised by Allabar and Nowak, following the order of their Comment sections.

2. Experimental design and effect on melt degassing

Allabar and Nowak argue that the use of glass powder as starting material for decompression experiments can lead to the formation of bubbles prior to decompression initiation, due to the entrapment of excess water or air during preparation, as discussed in Preuss et al. (2016).

Our sample preparation follows a similar procedure as in several laboratories (e.g., Pichavant et al., 2013; Le Gall and Pichavant, 2016, Fiege et al. 2014, Fiege and Chicy, 2015); more specifically, we followed two steps: first, the glass powder was subject to 300 MPa and 1200 °C for 24-48 h for hydration (or carbonation); then the hydrated/carbonated glass cylinders were equilibrated at 200 MPa and 1200 °C for additional 24-48 h, and then decompressed.

This procedure thus includes a long-time (24-48 h) step of hydration/carbonation at a pressure (300 MPa) much higher than the equilibrium and initial decompression pressure (200 MPa), thus ensuring the complete dissolution of the volatiles during the hydration/carbonation step. In this way, the H_2O and CO_2 contents used for hydration/carbonation were always lower than, or equal to (only in the supersaturated H_2O series), the saturation values at 300 MPa, thus preventing the formation of bubbles for excess H_2O or CO_2 in the starting material and hence in the glass cylinders used for decompression experiments. Moreover, we designed a pre-decompression phase of 48-96 h (typically >> 48 h), i.e., much longer than the 24 h interval after which Preuss et al. (2016) noticed the disappearance of potential problems related to the use of glass powder.

Actually, in our undecompressed glass cylinders, equilibrated at 200 MPa (namely D0; "Glasses directly quenched at $P_f = P_i$" in our paper), we documented the presence of bubbles, with minor values of porosity (0.03-0.3%) and *BND* (1–3.5 x 10^{11} m^{-3}, i.e., much lower than the peak *BND*s of 2-8 x 10^{12} m^{-3} obtained in decompressed samples) in D0 cases of all series (Table 1, this Reply),

including H_2O-rich (A and A2, mole fraction X_{H2O}=1), H_2O+CO_2-bearing (B, X_{H2O}=X_{CO2}=0.5) and CO_2-rich (C, X_{CO2}=1) melts. These are air bubbles (virtually 100% air), inherited by the tiny pore spaces present in the starting glass powders hydrated/carbonated at 300 MPa, which do not affect the experimental degassing process (e.g., H_2O and CO_2 nucleation; see following sections), due to their nature, amount and size.

2.1. Starting conditions and 2.2. Conditions just before decompression

The Authors of the Comment speculate that during the (pre-decompression) equilibration step at 200 MPa and 1200 °C for 24-48 h, the excess H_2O in the melt of the glass cylinders would start to diffuse into the pre-existing bubbles, or into potential fringe bubbles at the melt-capsule interface. They also calculate a diffusion timescale of water into pre-existing bubbles much faster than the 24-48 h of the equilibration step. Their intention is to demonstrate that our H_2O-saturated and oversaturated series (A and A2) contain "*identical amount of dissolved H_2O just before decompression, i.e. the equilibrium value of ~6 wt%, together with an excess fluid phase within the observed [pre-existing] bubbles in the sample volume with a BND of 1.1 x 10^{11} to 3.3 x 10^{11} m^{-3}. The amount of the excess fluid phase coexisting with the hydrous melt depends on the initial c_{H2Ot} [i.e., H_2O concentration] of the glass cylinders*".

The assumptions of Allabar and Nowak are speculative and unsupported by any evidence. In fact, if H_2O diffusion would occur from the melt toward pre-existing bubbles during the 24-48 h of equilibration at 200 MPa, we should observe a higher H_2O amount in the starting glass hydrated at 300 MPa with respect to the corresponding undecompressed samples equilibrated at 200 MPa. However, as we show in Table 1, it is evident that, if supersaturation is present in the pre-hydrated (at 300 MPa) glass, it is maintained in the corresponding glass cylinder quenched after 24-48 h of equilibrium at 200 MPa (see D0 of the oversaturated series A2 in Table 1). This consistently rules out H_2O or CO_2 loss at this stage, possibly due to the presence of air in the pre-existing bubbles that prevents H_2O (or CO_2) diffusion (see also section 2.3 below).

Moreover, pre-existing bubbles are also present in the H_2O- and/or CO_2-saturated series A, B, C (without volatile excess, Table 1), with similar porosity values (0.2-0.3%) in the saturated series C with pure CO_2 (dissolved CO_2 <1000 ppm) and in the H_2O oversaturated series A2 (some wt% of dissolved H_2O).

Series	Starting glass (at 300 MPa)	D0 (at 200 MPa)	Solubility at 200 MPa	Super-saturation before decompression	BND in D0 (m^{-3}) *Pre-existing bubbles*
A	***A-1***: H_2O = 5.8 (0.1) *TGA: H_2O = 5.3 (0.2)*	***a-0***: H_2O = 6.0 (0.1) *TGA: H_2O = 5.5 (0.1)*	H_2O = 6.0 [5.5*]	**$\Delta H_2O = 0$**	1.1 x 10^{11}
B	***B-1***: H_2O = 3.3 (0.1); CO_2 = 670 (90) *TGA: H_2O = 3.3 (0.1)*	***b-0***: H_2O = 3.5 (0.1); CO_2 = 670 (90) *TGA: H_2O = 3.10 (0.2)*	H_2O = 3.4 [3.0*]; CO_2 = 680 [493*]	ΔH_2O = 0.1; ΔCO_2 = -10	3.5 x 10^{11}
C	***C-1***: CO_2 = 970 (160)	***c-0***: CO_2 = 770 (160)	CO_2 = 872 [615*]	ΔCO_2 = -102	2.1 x 10^{11}
A2	***A2-5***: H_2O = 6.6 (0.2) *TGA: H_2O = 6.8 (0.10)*	***a2-0***: H_2O = 6.4 (0.2) *TGA: H_2O = 6.5 (0.10)*	H_2O = 6.0 [5.5*]	**$\Delta H_2O = 0.4$**	3.3 x 10^{11}

Table 1. *H_2O (wt%) and CO_2 (ppm), FTIR (Fourier Transform Infrared Spectroscopy) data with associated errors (in round brackets); for H_2O contents, TGA (thermogravimetry) data are also provided. Solubility data from Ghiorso and Gualda (2015) and Papale et al. (2006) (in square brackets; symbol *), the latter showing even lower solubility values. Overall, considering both FTIR and TGA measurements, undecompressed (D0) samples show higher H_2O contents in the H_2O oversaturated series A2 (i.e., 6.4-6.5 wt%) than in the H_2O-saturated series A (5.5-6.0 wt%).*

2.3 Degassing during decompression

Allabar and Nowak assume that, during decompression in our H_2O-rich series (A and A2), the exsolved H_2O would diffuse into the pre-existing bubbles, thus preventing the increment of the H_2O supersaturation in the melt, required for the homogeneous nucleation of H_2O bubbles. On these grounds, and with the aim to prove their assumptions, they apply a model for bubble growth in magmas (Coumans et al., 2020) to simulate the degassing process in a bubby melt, using the following starting conditions: an initial H_2O content (H_2O_i) corresponding to the saturation value at P_i, and our porosity and *BND* data attributed to pre-existing bubbles. The results of their model show that, up to 100 MPa, pre-existing bubbles grow following equilibrium degassing under slow decompression (0.01 MPa s^{-1}), preventing H_2O supersaturation in the melt and nucleation of new bubbles; by contrast, during fast decompression (1 MPa s^{-1}), these bubbles can only grow in disequilibrium conditions, thus allowing H_2O supersaturation in the melt (between 0.5 and 0.2 wt% at 150 MPa, as a function of the adopted *BND*) and homogeneous bubble nucleation. The result of this last simulation invalidates (at least for 1 MPa/s simulations) the Allabar and Nowak's hypothesis for a fast decrement of melt supersaturation due to water diffusion toward pre-existing

bubbles. In fact, after 50 MPa of decompression, H_2O supersaturation is still effective in the melt. Moreover, from these calculations, the *BND* values would be expected to remain constant during slow decompression (absence of bubble nucleation), while they should increase during fast decompression (occurrence of bubble nucleation). However, our experimental data show an increase of the *BND* values up to 100 MPa irrespective of the decompression rate, thus the above calculations might only justify the *BND* trends observed in our fast decompression experiments, while they are inconsistent with our slow decompression experiments. To solve this discrepancy in their model calculations, Allabar and Nowak hypothesize that the supersaturation achieved in fast decompression simulations would be unable to drive bubble nucleation, and that the *BND* increase (observed in both series A and A2, at both decompression rates) would not be effective, and rather due to the detection limit of our textural analysis.

Thus, again, Allabar and Nowak do not take care to verify their assumptions in light of the actual data from our experimental samples, i.e.:

- at both slow and fast decompression rates, measured *BND*s clearly increase up to a maximum value, before the degree of H_2O supersaturation falls below a critical threshold, consistent with the CNT;

- the H_2O content at a final pressure of 150 MPa is higher than the solubility value, indicating that water exsolution is delayed until the energetic barrier for the formation of the new phase boundary is exceeded by the achievement of the critical supersaturation pressure required to trigger homogeneous bubble nucleation (ΔP_{HoN});

- textural and chemical data also clearly indicate a second nucleation event during fast decompression at low final pressures, which cannot be explained using the Authors' hypothesis (see details in our original paper and Fig. 1 and 2a therein).

On these grounds, it seems that the Authors of the Comment do not properly consider all the assumptions of the Coumans et al. (2020)'s model when applied to simulating our experimental results. In fact, this is a bubble growth model that does not take into account the bubble formation processes and assumes that H_2O bubbles (i.e., 100% H_2O) are already nucleated in the melt. Accordingly, the boundary conditions of the model imply that the concentration of dissolved H_2O at the bubble-melt interface equals the solubility value (since the chemical potentials of H_2O in the bubbles and in the melt must be equal); when the H_2O concentration at the midpoint between two bubbles exceeds the solubility value, a H_2O gradient is generated, which drives water diffusion. Since in our experiments pre-existing bubbles are not related to excess H_2O (being, instead, air-dominated), the model is not suitable to reproduce our experimental data and, consequently, cannot invalidate the clear evidence for homogeneous bubble nucleation.

197

198 ***2.4 The observed increase in BND during decompression despite the absent driving force for***
199 ***bubble formation***

200 In our paper, we analysed *BND* and bubble size distribution (BDS) by means of X-ray computed
201 microtomography (micro-CT) technique, which allows detecting at high resolution the whole
202 volume of experimental samples that remain intact and available for future analyses. Since the used
203 3D microscope (Xradia 410 Versa) can reach a resolution up to 0.9 μm, a preliminary study has
204 been conducted on selected experimental samples to choose the best (cost/benefit) analytical
205 conditions. Pilot samples were explored at different resolutions (i.e., 4, 2 and 1 μm), implying
206 longer scans and smaller sample volume investigated with increasing resolution. Generally, we
207 obtained negligible differences in *BND*s and BSDs resulting from the different resolution scans;
208 however, the minor differences observed by Allabar and Nowak are reasonably due to the intrinsic
209 heterogeneity of the sample, as the different resolution scans detected different sub-volumes.
210 Based on these preliminary inspections, we chose to scan the whole sample volumes at 4 μm
211 resolution, as the cumulative BSD curves flatten toward the small bubble sizes to form a plateau,
212 thus indicating that bubbles of the finer size tail do not affect significantly the *BND* values. BSDs,
213 shown in Fig. 1 and Fig. 2 for different resolution scans, both for D0 (undecompressed) samples
214 and for samples where the nucleation peak is reached (P_f of 100 MPa in series A and 150 MPa in
215 series A2; P_f of 25-50 MPa for series B and C), clearly indicate that the curves flatten toward finer
216 bubble sizes, leading to similar *BND*s for the different resolutions. Moreover, the BND values
217 obtained from D0 runs are much lower than the maximum *BND*s achieved from the corresponding
218 series decompressed at lower final pressures at both low and fast rates (Fig. 1 and Fig. 2 in this
219 Reply), thus consistently indicating the nucleation of new bubbles.
220 Additionally, we point out that the transmitted light microscopy technique mentioned by Allabar
221 and Nowak allows the investigation of very small sample volumes (i.e., in the order of 0.00058
222 mm^3 - 0.0057 mm^3), and thus it is usually employed for samples bearing very small (1-5 μm-sized)
223 bubbles (see Allabar and Nowak, 2018) or, in case of samples that also contain larger (> 5 μm)
224 bubbles, is accompanied by 2D (e.g., scanning electron microscope) analyses, to account for the
225 well-known *intersection-probability* (the higher probability of intersecting large objects than
226 smaller ones in any random section) and *cut-section* (any random section through a rock texture
227 probably intersects, for each individual object, a smaller section than the true 3D size) effects
228 (Higgins et al., 2000; 2006).
229 Instead, 3D analyses by means of high resolution computed microtomography allow the
230 investigation of larger sample volumes (e.g., even the whole sample volume in case of 4 μm

resolution scan, up to 50 mm^3 at 2 µm resolution, and up to 3 mm^3 at 1 µm resolution) and need neither calibration nor stereological corrections, as they directly measure the real 3D texture of samples. This is a crucial aspect, as tiny bubbles are generally not homogeneously distributed in the sample, so that the inspection of a very small subvolume might be not representative of the whole sample texture. In this regard, we suggest to calibrate light microscopy analyses with high-resolution micro-CT, to obtain representative quantitative (including bubble number, as well as size, shape, spatial coordinates) results.

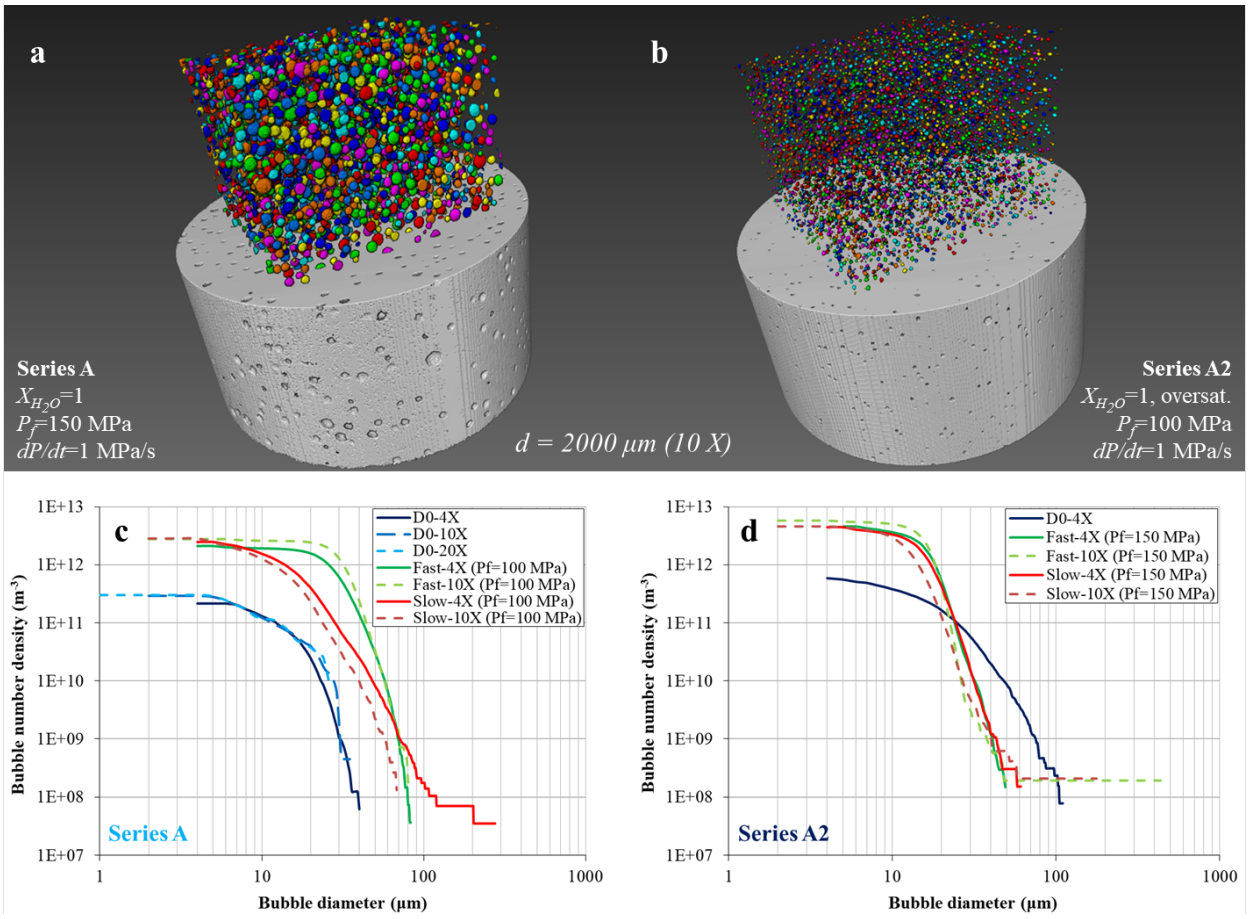

Fig. 1. *3D volume rendering and Cumulative Bubble Size Distributions for series A (a, c) and A2 (b, d). (a, b) 3D volume rendering for samples where the maximum BND is achieved. (c,d) Cumulative Bubble Size Distributions for D0 (undecompressed samples) and samples where the maximum BND is achieved in the corresponding series at both decompression rates, obtained from 3D images at different resolutions (4, 2 and 1 µm for 4X, 10X and 20X scans, respectively).*

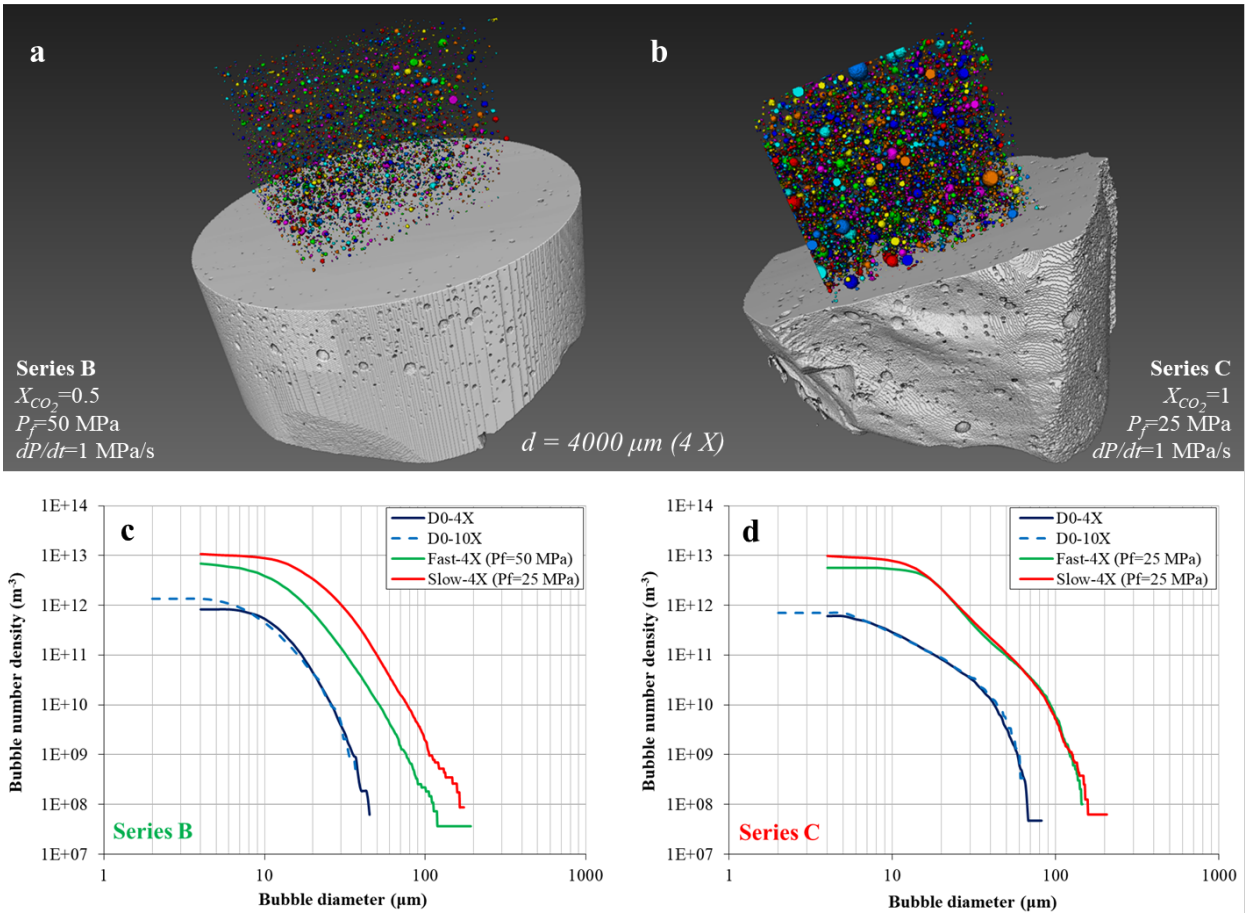

Fig. 2. *3D volume rendering and Cumulative Bubble Size Distributions for series B (a, c) and C (b, d). (a, b) 3D volume rendering for samples where the maximum BND is achieved. (c,d) Cumulative Bubble Size Distributions for D0 (undecompressed samples) and samples where the maximum BND is achieved in the corresponding series at both decompression rates, obtained from 3D images at different resolutions (4, 2 and 1 µm for 4X, 10X and 20X scans respectively).*

3. Supersaturation required for bubble formation

3.1 ΔP_{HoN} vs. $\Delta P_{Pi\text{-}PHoN}$

Allabar and Nowak observe that our series A experiments show a supersaturation pressure required for homogeneous bubble nucleation ($\Delta P_{HoN} = P_{SAT} - P_{HoN}$, where P_{SAT} is the saturation pressure and P_{HoN} is the nucleation pressure) ≤ 50 MPa, i.e., within the range of values reported in literature for evolved alkaline melts (ΔP_{HoN} between < 50 and 112 MPa). They report that, for a more detailed comparison with literature data, we also used the parameter $\Delta P_{Pi\text{-}PHoN}$ (= P_i - P_{HoN}, where P_i is the initial decompression pressure) and that we observed a negative correlation of both ΔP_{HoN} *and* $\Delta P_{Pi\text{-}PHoN}$ with the initial content of dissolved H_2O (H_2O_i). However, they find the use of these two parameters confusing and contest the use of $\Delta P_{Pi\text{-}PHoN}$ (as it depends on the choice of P_i,)

in experiments with initial H_2O-undersaturated conditions, to discuss the nucleation theory in terms of the degree of supersaturation.

Actually, in their Discussion, the Authors of the Comment misunderstand the aim of our discussion on ΔP_{HoN} and $\Delta P_{Pi\text{-}PHoN}$. As specified in our paper, we used the parameter $\Delta P_{Pi\text{-}PHoN}$ to compare the results of experiments with the same P_i (this parameter was also reported with different symbols as a function of P_i in Fig. 6c; see also below) and T. Therefore, when $\Delta P_{Pi\text{-}PHoN}$ is combined with the initial H_2O content, it is obviously function of the supersaturation degree (i.e., for a given P_i, melts with higher H_2O_i require lower $\Delta P_{Pi\text{-}PHoN}$ to nucleate bubbles; see also Fig. 3 of the Comment). Moreover, contrary to what stated in the Comment, we did not use the observed H_2O_i *vs.* $\Delta P_{Pi\text{-}PHoN}$ relationship to discriminate the nucleation mechanisms. Instead, we combined several evidence (from literature and our novel data) supporting a "*direct relationship between nucleation and supersaturation degree, thus supporting CNT, i.e.: (i) the negative correlation between* $\Delta P_{Pi\text{-}PHoN}$ *and* H_2O_i*, starting from similar* P_i *[…]; (ii) the progressive increase in BND (and* D_m*) with decreasing* P_f*, up to a peak BND reached when the degree of supersaturation falls below the threshold value for further nucleation […]; (iii) the occurrence of a second nucleation events achieved in our experiments on* H_2O*-rich melts at high dP/dt, likely due to short decompression time for efficient* H_2O *diffusion, implying the restoration of an adequate degree of supersaturation for nucleation […]*" (see the second paragraph of section 3.1.1.3 of the paper, cited by the Authors).

3.2 ΔP_{HoN} *vs. initial* H_2O *concentration of the melt*

Allabar and Nowak arbitrarily select a sub-set of data from the complete experimental database available from literature for evolved alkaline melts, to examine the above described dependence of ΔP_{HoN} from H_2O_i. Based on this limited dataset, they find a positive correlation of ΔP_{HoN} (ranging 40-90 MPa) *vs.* H_2O_i. Also, they report that the value of ΔP_{HoN} in K-phonolite (~ 90 MPa, for H_2O_i ~5 wt%; Allabar et al., 2020a) differs with respect to Na-phonolite (~ 60 MPa, for H_2O_i ~5 wt%; Gardner et al., 2012), but suggest that this difference might be unrealistic, due to H_2O resorption from bubbles during the (post-decompression) isobaric quench, leading to overestimations of ΔP_{HoN}. However, they attribute a ΔP_{HoN} value for our trachytic melts lower than that actually reported in our paper (ΔP_{HoN} ~ 50 MPa, for H_2O_i ~6 wt%, i.e., within the ≤ 50-112 MPa range of literature values for evolved alkaline melts), providing no explanation for this arbitrary calculation (see Fig. 4 of their Comment).

The Authors of the Comment thus claim for a positive correlation between ΔP_{HoN} and H_2O_i, opposite to our findings. Here, we highlight that their correlation (black curve in Fig. 4 of the

Comment) is based on just three data points (open circles in their Fig. 4) resulting from their recent paper on K-phonolitic melts (Allabar et al., 2020a), although they try arbitrarily to extend this relationship to all evolved alkaline melts. Following the Allabar and Nowak' reasoning, we note that, if the ΔP_{HoN} estimates might be compromised by H_2O resorption, this should be particularly true for their set of decompressed samples (Allabar et al., 2020a). In fact, their decompressed samples always show residual H_2O content identical to the initial H_2O values (i.e., H_2O_i before decompression) up to low final pressures; this anomalous behaviour is justified by invoking H_2O resorption from bubbles back into the melt during quenching with a low cooling rate (Allabar et al., 2020b). However, this H_2O resorption would affect not only the water content (and then ΔP_{HoN}), but also the BND values, on which the Authors of the Comment base their hypothesis of spinodal decomposition.

Surprisingly, in discussing the alleged ΔP_{HoN} *vs.* H_2O_i correlation, they ignore not only the data on Na-phonolites (ΔP_{HoN} ~ 60 MPa, H_2O_i~5 wt%; Gardner et al., 2012) but also the data on K-phonolites derived from melt composition and experimental conditions identical to those of Allabar et al. (2020a): e.g., $\Delta P_{HoN} \leq 60$ MPa, for H_2O_i ~5 wt% (Preuss et al., 2016); $\Delta P_{HoN} \leq 50$ MPa, for H_2O_i ~5.5-6 wt% (Marxer et al., 2015). Also, our results on trachytic melts (ΔP_{HoN} ~ 50 MPa, for H_2O_i of 6 wt%) closely match available literature data on evolved alkaline melts.

Finally, the Authors of the Comment misunderstand the aim of our discussion on the ΔP_{HoN} *vs.* H_2O_i relationship. They state that "*To discuss bubble formation (e.g., to discriminate between nucleation or spinodal decomposition), however, the dependence of* ΔP_{HoN} *as a function of initial* H_2O *concentration [*$H2O_i$*] is required*"; however, they do not provide information about how this relationship (either positive or negative) can allow discriminating between the two mechanisms.

In our paper, the ΔP_{HoN} *vs.* H_2O_i relationship was actually introduced to investigate the factors controlling the wide range of ΔP_{HoN} values (from ≤ 50 to 112 MPa) observed in evolved alkaline melts, rather than distinguish between the nucleation mechanisms. Using the complete database available for these melts (obtained by updating the pre-existing database of Shea, 2017) we found that the "ΔC_{HoN} *[supersaturation concentration, i.e., ratio between the* H_2O_i *and* H_2O *saturation concentration at* P_{HoN}*] required for nucleation can sharply increase in melts with low initial* H_2O *content (Fig. 6a; e.g.,* ΔC_{HoN} *= 1.1–1.3 for* H_2O_i *> 5.5 wt%; 1.2–1.7 for* H_2O_i *= 4.5–5.5; 1.5–2.5 for* H_2Oi *< 4.5 wt%), resulting in higher* ΔP_{HoN} *(Fig. 6b). This suggests that the surface tension in evolved alkaline melts increases as the initial* H_2O *content decreases, according to previous experimental and modeling studies (e.g., Khitarov et al., 1979; Bagdassarov et al., 2000; Gardner et al., 2013; Colucci et al., 2016)*" (see the third paragraph of section 3.1.1.1.1 in our paper; see also Fig. 3 in this Reply). In fact, the CNT (in contrast to the spinodal decomposition) states that (for a

given melt composition) ΔP_{HoN} is controlled by the surface tension: i.e., with higher surface tension (i.e., for lower H_2O_i), a higher ΔP_{HoN} is required (Fig. 3). Thus, the surface tension appears as the main controlling factor of the H_2O_i *vs.* ΔP_{HoN} relationship.

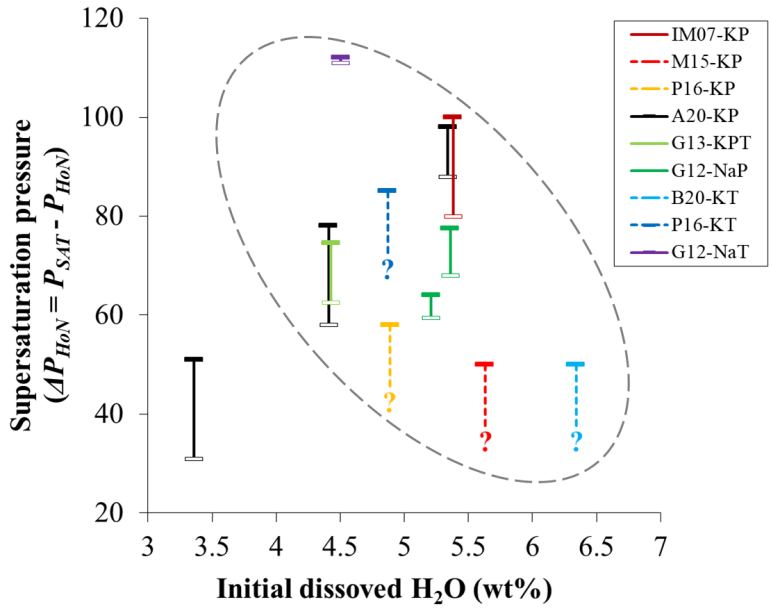

Fig. 3. *Supersaturation pressure ($\Delta P_{HoN} = P_{SAT} - P_{HoN}$), vs. initial dissolved H_2O content (H_2O_i). Using the complete database for evolved alkaline melts, a roughly negative H_2O_i-ΔP_{HoN} correlation is shown (dashed grey area), besides a single outlier. Conversely, the Authors of the Comment claim for a positive correlation, by arbitrarily selecting just the three data points of their paper on K-phonolitic melts (Allabar et al., 2020a; black symbols). As, during experiments, samples are not decompressed continuously, yet for defined ΔP steps, for each sample we consider a range of ΔP_{HoN} values, between a maximum ΔP_{HoN} (corresponding to the highest P_f at which bubbles appear in the samples; closed symbols) and a minimum ΔP_{HoN} (corresponding to the lowest P_f at which bubbles do not yet appear; open symbols). For samples decompressed by wider ΔP steps, only the maximum value of ΔP_{HoN} (closed symbols) is obtained, whereas the minimum ΔP_{HoN}, is not constrained (uncertainty shown by dashed lines and "?" symbol). In our experiments (B20) a ΔP_{HoN} ~ 50 MPa is suggested by an incipient nucleation event after a pressure decrease of 50 MPa at initial saturation conditions (see the original paper for details). KP and NaP: K- and Na-phonolites; KT and NaT: K- and Na-trachytes; KPT: K-phonotephrite. References: Iacono-Marziano et al. (2007; IM07); Gardner (2012; G12); Gardner et al. (2013; G13); Marxer et al., (2015; M15); Preuss et al. (2016; P16); Allabar et al. (2020a) (A20); our paper (B20). Data where the uncertainty in*

ΔP_{HoN} range is ≥ 100 MPa, are not plotted, as they span the whole ΔP_{HoN} interval for literature data on evolved alkaline melts.

4. Final remarks

In our paper (Buono et al., 2020), we presented a systematic study to fully constrain the degassing behaviour (e.g., bubble nucleation and growth, degassing styles and regimes) of evolved alkaline melts, over a wide range of variables (e.g., H_2O and CO_2 contents, final pressures, decompression rates, temperatures), based on a comprehensive review of previous experimental works, in light of novel experimental findings.

In their Comment, Allabar and Nowak, make an arbitrary selection of our new experimental results (i.e., those concerning bubble nucleation in H_2O-rich melts), to conclude that the classical nucleation theory, widely accepted in literature to explain homogeneous bubble nucleation in magmas, cannot be applied to evolved alkaline compositions, in which nucleation would instead take place by spinodal decomposition. In our opinion, they do not provide further supporting evidence for their claims; the epistemic framework employed by these Authors appears to be hypothetico-deductivism, in that a hypothesis was formulated *a priori* rather than based on experimental evidence.

References

Allabar, A., Nowak, M., 2018. Message in a bottle: Spontaneous phase separation of hydrous Vesuvius melt even at low decompression rates. Earth Planet. Sci. Lett. 501, 192–201. https://doi.org/10.1016/j.epsl.2018.08.047.

Allabar, A., Dobson, K.J., Bauer, C.C., Nowak, M., 2020a. Vesicle shrinkage in hydrous phonolitic melt during cooling. Contrib. Mineral. Petrol., 175, 21. https://doi.org/10.1007/s00410-020-1658-3.

Allabar, A., Salis Gross, E., Nowak, M., 2020b. The effect of initial H_2O concentration on decompression-induced phase separation and degassing of hydrous phonolitic melt. Contrib. Mineral. Petrol. 175, 22. https://doi.org/10.1007/s00410-020-1659-2.

Bagdassarov, N., Dorfman, A., Dingwell, D., 2000. Effect of alkalis, phosphorus, and water on the surface tension of haplogranite melt. Am. Mineral. 85, 33–40. https://doi.org/10.2138/am-2000-0105.

392 Buono, G., Fanara, S., Macedonio, G., Palladino, D.M., Petrosino, P., Sottili, G., Pappalardo, L.,
393 2020. Dynamics of degassing in evolved alkaline magmas: Petrological, experimental and
394 theoretical insights. Earth-Sci. Rev. 211, 103402. https://doi.org/10.1016/j.earscirev.2020.103402.
395 Colucci, S., Battaglia, M., Trigila, R., 2016. A thermodynamical model for the surface tension of
396 silicate melts in contact with H_2O gas. Geochim. Cosmochim. Acta 175, 113–127.
397 https://doi.org/10.1016/j.gca.2015.10.037.
398 Coumans, J.P., Llewellin, E.W., Wadsworth, F.B., Humphreys, M.C.S., Mathias, S.A., Yelverton,
399 B.M., Gardner, J.E., 2020. An experimentally validated numerical model for bubble growth in
400 magma. J. Volcanol. Geotherm. Res. 402, 107002.
401 https://doi.org/10.1016/j.jvolgeores.2020.107002.
402 Fiege, A., Cichy, S.B., 2015. Experimental constraints on bubble formation and growth during
403 magma ascent: a review. Am. Mineral. 100, 2426–2442. https://doi.org/10.2138/am-2015-5296.
404 Fiege, A., Holtz, F., Cichy, S.B., 2014. Bubble formation during decompression of andesitic
405 melts. Am. Mineral. 99, 1052–1062. http://dx.doi.org/10.2138/am.2014.4719.
406 Gardner, J.E., 2012. Surface tension and bubble nucleation in phonolite magmas. Geochim.
407 Cosmochim. Acta 76, 93–102. https://doi.org/10.1016/j.gca.2011.10.017.
408 Gardner, J.E., Ketcham, R.A., Moore, G., 2013. Surface tension of hydrous silicate melts:
409 constraints on the impact of melt composition. J. Volcanol. Geotherm. Res. 267, 68–74.
410 https://doi.org/10.1016/j.jvolgeores.2013.09.007.
411 Ghiorso, M.S., Gualda, G.A.R., 2015. A H_2O–CO_2 mixed fluid saturation model compatible with
412 rhyolite-MELTS. Contrib. Mineral. Petrol. 169, 1245. https://doi.org/10.1007/s00410-015-1141-8.
413 Gonnermann, H.M., Manga, M., 2007. The fluid mechanics inside a volcano. Annu. Rev. Fluid
414 Mech. 39, 321–356. https://doi.org/10.1146/annurev.fluid.39.050905.110207.
415 Gonnermann, H.M., Manga, M., 2012. Dynamics of magma ascent in the volcanic conduit, in:
416 Fagents, S.A., Gregg, T.K.P., Lopes, R.M.C. (Eds.), Modeling Volcanic Processes. Cambridge
417 University Press, Cambridge, pp. 55–84. https://doi.org/10.1017/CBO9781139021562.004.
418 Higgins, M.D., 2000. Measurement of Crystal Size Distributions. Am. Mineral. 85, 1105-1116.
419 https://doi.org/10.2138/am-2000-8-901.
420 Higgins, M.D., 2006. Quantitative textural measurements in igneous and metamorphic petrology.
421 Cambridge University Press, Cambridge. https://doi.org/10.1017/CBO9780511535574.
422 Iacono-Marziano, G., Schmidt, B.C., Dolfi, D., 2007. Equilibrium and disequilibrium degassing of
423 a phonolitic melt (Vesuvius AD 79 “white pumice”) simulated by decompression experiments. J.
424 Volcanol. Geotherm. Res. 161, 151–164. https://doi.org/10.1016/j.jvolgeores.2006.12.001.

425 Khitarov, N.I., Lebedev, Y.B., Dorfman, A.M., Bagdasarov, N.S., 1979. Effects of temperature,
426 pressure and volatiles on the surface tension of molten basalt. Geochem. Int. 16, 78–86.
427 Le Gall, N., Pichavant, M., 2016. Homogeneous bubble nucleation in H_2O- and H_2O-CO_2-bearing
428 basaltic melts: results of high temperature decompression experiments. J. Volcanol. Geotherm. Res.
429 327, 604–621. https://doi.org/10.1016/j.jvolgeores.2016.10.004.
430 Marxer, H., Bellucci, P., Nowak, M., 2015. Degassing of H_2O in a phonolitic melt: a closer look at
431 decompression experiments. J. Volcanol. Geotherm. Res. 297, 109–124.
432 https://doi.org/10.1016/j.jvolgeores.2014.11.017.
433 Navon, O., Lyakhovsky, V., 1998. Vesiculation processes in silicic magmas. Geol. Soc. London
434 Spec. Pub. 145, 27–50. https://doi.org/10.1144/GSL.SP.1996.145.01.03.
435 Papale P., Moretti R., Barbato D., 2006. The compositional dependence of the saturation surface
436 of H_2O+CO_2 fluids in silicate melts. Chem. Geol. 229, 78–95.
437 https://doi.org/10.1016/j.chemgeo.2006.01.013.
438 Pichavant, M., Di Carlo, I., Rotolo, S.G., Scaillet, B., Burgisser, A., Le Gall, N., Martel, C., 2013.
439 Generation of CO_2-rich melts during basalt magma ascent and degassing. Contrib. Mineral. Petrol.
440 166, 545–561. https://doi.org/10.1007/s00410-013-0890-5.
441 Preuss, O., Marxer, H., Ulmer, S., Wolf, J., Nowak, M., 2016. Degassing of hydrous trachytic
442 Campi Flegrei and phonolitic Vesuvius melts: experimental limitations and chances to study
443 homogeneous bubble nucleation. Am. Mineral. 101, 859–875. https://doi.org/10.2138/am-2016-
444 5480.
445 Sparks, R.S.J, 1978. The dynamics of bubble formation and growth in magmas: a review and
446 analysis. J. Volcanol. Geotherm. Res. 3, 1–37. https://doi.org/10.1016/0377-0273(78)90002-1.
447 Sparks, R.S.J., Barclay, J., Jaupart, C., Mader, H.M., Phillips, J.C., 1994. Physical aspects of
448 magmatic degassing. I. Experimental and theoretical constraints on vesiculation. Rev. Mineral.
449 Geochem. 30, 413–445.
450 Toramaru, A., 1995. Numerical study of nucleation and growth of bubbles in viscous magmas. J.
451 Geophys. Res. 100, 1913–1931. https://doi.org/10.1029/94JB02775.
452 Toramaru, A., 2006. BND (bubble number density) decompression rate meter for explosive
453 volcanic eruptions. J. Volcanol. Geotherm. Res. 154, 303–316.
454 https://doi.org/10.1016/j.jvolgeores.2006.03.027.